Eur. Phys. J. C 2, 77–93 (1998)

THE EUROPEAN PHYSICAL JOURNAL C
© Springer-Verlag 1998

Charged particles and neutral kaons in photoproduced jets at HERA

ZEUS Collaboration

J. Breitweg, M. Derrick, D. Krakauer, S. Magill, D. Mikunas, B. Musgrave, J. Repond, R. Stanek, R.L. Talaga, R. Yoshida, H. Zhang
Argonne National Laboratory, Argonne, IL, USA[p]

M.C.K. Mattingly
Andrews University, Berrien Springs, MI, USA

F. Anselmo, P. Antonioli, G. Bari, M. Basile, L. Bellagamba, D. Boscherini, A. Bruni, G. Bruni, G. Cara Romeo, G. Castellini[1], L. Cifarelli[2], F. Cindolo, A. Contin, M. Corradi, S. De Pasquale, I. Gialas[3], P. Giusti, G. Iacobucci, G. Laurenti, G. Levi, A. Margotti, T. Massam, R. Nania, F. Palmonari, A. Pesci, A. Polini, F. Ricci, G. Sartorelli, Y. Zamora Garcia[4], A. Zichichi
University and INFN Bologna, Bologna, Italy[f]

C. Amelung, A. Bornheim, I. Brock, K. Coböken, J. Crittenden, R. Deffner, M. Eckert, M. Grothe, H. Hartmann, K. Heinloth, L. Heinz, E. Hilger, H.-P. Jakob, U.F. Katz, R. Kerger, E. Paul, M. Pfeiffer, Ch. Rembser[5], J. Stamm, R. Wedemeyer[6], H. Wieber
Physikalisches Institut der Universität Bonn, Bonn, Germany[c]

D.S. Bailey, S. Campbell-Robson, W.N. Cottingham, B. Foster, R. Hall-Wilton, M.E. Hayes, G.P. Heath, H.F. Heath, J.D. McFall, D. Piccioni, D.G. Roff, R.J. Tapper
H.H. Wills Physics Laboratory, University of Bristol, Bristol, UK[o]

M. Arneodo[7], R. Ayad, M. Capua, A. Garfagnini, L. Iannotti, M. Schioppa, G. Susinno
Calabria University, Physics Department and INFN, Cosenza, Italy[f]

J.Y. Kim, J.H. Lee, I.T. Lim, M.Y. Pac[8]
Chonnam National University, Kwangju, Korea[h]

A. Caldwell[9], N. Cartiglia, Z. Jing, W. Liu, B. Mellado, J.A. Parsons, S. Ritz[10], S. Sampson, F. Sciulli, P.B. Straub, Q. Zhu
Columbia University, Nevis Labs., Irvington on Hudson, N.Y., USA[q]

P. Borzemski, J. Chwastowski, A. Eskreys, J. Figiel, K. Klimek, M.B. Przybycień, L. Zawiejski
Institute of Nuclear Physics, Cracow, Poland[j]

L. Adamczyk[11], B. Bednarek, M. Bukowy, A. Czermak, K. Jeleń, D. Kisielewska, T. Kowalski, M. Przybycień, E. Rulikowska-Zarębska, L. Suszycki, J. Zając
Faculty of Physics and Nuclear Techniques, Academy of Mining and Metallurgy, Cracow, Poland[j]

Z. Duliński, A. Kotański
Jagellonian University , Department of Physics, Cracow, Poland[k]

G. Abbiendi[12], L.A.T. Bauerdick, U. Behrens, H. Beier, J.K. Bienlein, G. Cases[13], O. Deppe, K. Desler, G. Drews, U. Fricke, D.J. Gilkinson, C. Glasman, P. Göttlicher, T. Haas, W. Hain, D. Hasell, K.F. Johnson[14], M. Kasemann, W. Koch, U. Kötz, H. Kowalski, J. Labs, L. Lindemann, B. Löhr, M. Löwe[15], O. Mańczak, J. Milewski, T. Monteiro[16], J.S.T. Ng[17], D. Notz, K. Ohrenberg[18], I.H. Park[19], A. Pellegrino, F. Pelucchi, K. Piotrzkowski, M. Roco[20], M. Rohde, J. Roldán, J.J. Ryan, A.A. Savin, U. Schneekloth, O. Schwarzer, F. Selonke, B. Surrow, E. Tassi, T. Voß[21], D. Westphal, G. Wolf, U. Wollmer[22], C. Youngman, A.F. Żarnecki, W. Zeuner
Deutsches Elektronen-Synchrotron DESY, Hamburg, Germany

B.D. Burow, H.J. Grabosch, A. Meyer, S. Schlenstedt
DESY-IfH Zeuthen, Zeuthen, Germany

G. Barbagli, E. Gallo, P. Pelfer
University and INFN, Florence, Italy[f]

G. Maccarrone, L. Votano
INFN, Laboratori Nazionali di Frascati, Frascati, Italy[f]

A. Bamberger, S. Eisenhardt, P. Markun, T. Trefzger[23], S. Wölfle
Fakultät für Physik der Universität Freiburg i.Br., Freiburg i.Br., Germany[c]

J.T. Bromley, N.H. Brook, P.J. Bussey, A.T. Doyle, N. Macdonald, D.H. Saxon, L.E. Sinclair, E. Strickland, R. Waugh, A.S. Wilson
Department of Physics and Astronomy, University of Glasgow, Glasgow, UK[o]

I. Bohnet, N. Gendner, U. Holm, A. Meyer-Larsen, H. Salehi, K. Wick
Hamburg University, I. Institute of Exp. Physics, Hamburg, Germany[c]

L.K. Gladilin[24], D. Horstmann, D. Kçira[25], R. Klanner, E. Lohrmann, G. Poelz, W. Schott[26], F. Zetsche
Hamburg University, II. Institute of Exp. Physics, Hamburg, Germany[c]

T.C. Bacon, I. Butterworth, J.E. Cole, G. Howell, B.H.Y. Hung, L. Lamberti[27], K.R. Long, D.B. Miller, N. Pavel, A. Prinias[28], J.K. Sedgbeer, D. Sideris, R. Walker
Imperial College London, High Energy Nuclear Physics Group, London, UK[o]

U. Mallik, S.M. Wang, J.T. Wu
University of Iowa, Physics and Astronomy Department , Iowa City, USA[p]

P. Cloth, D. Filges
Forschungszentrum Jülich, Institut für Kernphysik, Jülich, Germany

J.I. Fleck[5], T. Ishii, M. Kuze, I. Suzuki[29], K. Tokushuku, S. Yamada, K. Yamauchi, Y. Yamazaki[30]
Institute of Particle and Nuclear Studies, KEK, Tsukuba, Japan[g]

S.J. Hong, S.B. Lee, S.W. Nam[31], S.K. Park
Korea University, Seoul, Korea[h]

F. Barreiro, J.P. Fernández, G. García, R. Graciani, J.M. Hernández, L. Hervás[5], L. Labarga, M. Martínez, J. del Peso, J. Puga, J. Terrón[32], J.F. de Trocóniz
Universidad Autónoma Madrid, Depto de Física Teórica, Madrid, Spain[n]

F. Corriveau, D.S. Hanna, J. Hartmann, L.W. Hung, W.N. Murray, A. Ochs, M. Riveline, D.G. Stairs, M. St-Laurent, R. Ullmann
McGill University, Department of Physics, Montréal, Québec, Canada[a], [b]

T. Tsurugai
Meiji Gakuin University, Faculty of General Education, Yokohama, Japan

V. Bashkirov, B.A. Dolgoshein, A. Stifutkin
Moscow Engineering Physics Institute, Moscow, Russia[l]

G.L. Bashindzhagyan, P.F. Ermolov, Yu.A. Golubkov, L.A. Khein, N.A. Korotkova, I.A. Korzhavina, V.A. Kuzmin, O.Yu. Lukina, A.S. Proskuryakov, L.M. Shcheglova[33], A.N. Solomin[33], S.A. Zotkin
Moscow State University, Institute of Nuclear Physics, Moscow, Russia[m]

C. Bokel, M. Botje, N. Brümmer, F. Chlebana[20], J. Engelen, E. Koffeman, P. Kooijman, A. van Sighem, H. Tiecke, N. Tuning, W. Verkerke, J. Vossebeld, M. Vreeswijk[5], L. Wiggers, E. de Wolf
NIKHEF and University of Amsterdam, Amsterdam, Netherlands[i]

D. Acosta, B. Bylsma, L.S. Durkin, J. Gilmore, C.M. Ginsburg, C.L. Kim, T.Y. Ling, P. Nylander, T.A. Romanowski[34]
Ohio State University, Physics Department, Columbus, Ohio, USA[p]

H.E. Blaikley, R.J. Cashmore, A.M. Cooper-Sarkar, R.C.E. Devenish, J.K. Edmonds, J. Große-Knetter[35], N. Harnew, C. Nath, V.A. Noyes[36], A. Quadt, O. Ruske, J.R. Tickner[28], H. Uijterwaal, R. Walczak, D.S. Waters
Department of Physics, University of Oxford, Oxford, UK[o]

A. Bertolin, R. Brugnera, R. Carlin, F. Dal Corso, U. Dosselli, S. Limentani, M. Morandin, M. Posocco, L. Stanco, R. Stroili, C. Voci
Dipartimento di Fisica dell' Università and INFN, Padova, Italy[f]

J. Bulmahn, B.Y. Oh, J.R. Okrasiński, W.S. Toothacker, J.J. Whitmore
Pennsylvania State University, Department of Physics, University Park, PA, USA[q]

Y. Iga
Polytechnic University, Sagamihara, Japan[g]

G. D'Agostini, G. Marini, A. Nigro, M. Raso
Dipartimento di Fisica, University 'La Sapienza' and INFN, Rome, Italy[f]

J.C. Hart, N.A. McCubbin, T.P. Shah
Rutherford Appleton Laboratory, Chilton, Didcot, Oxon, UK[o]

D. Epperson, C. Heusch, J.T. Rahn, H.F.-W. Sadrozinski, A. Seiden, R. Wichmann, D.C. Williams
University of California, Santa Cruz, CA, USA[p]

H. Abramowicz[37], G. Briskin, S. Dagan[37], S. Kananov[37], A. Levy[37]
Raymond and Beverly Sackler Faculty of Exact Sciences, School of Physics, Tel-Aviv University,
Tel-Aviv, Israel[e]

T. Abe, T. Fusayasu, M. Inuzuka, K. Nagano, K. Umemori, T. Yamashita
Department of Physics, University of Tokyo, Tokyo, Japan[g]

R. Hamatsu, T. Hirose, K. Homma[38], S. Kitamura[39], T. Matsushita
Tokyo Metropolitan University, Department of Physics, Tokyo, Japan[g]

R. Cirio, M. Costa, M.I. Ferrero, S. Maselli, V. Monaco, C. Peroni, M.C. Petrucci, M. Ruspa, R. Sacchi, A. Solano, A. Staiano
Università di Torino, Dipartimento di Fisica Sperimentale and INFN, Torino, Italy[f]

M. Dardo
II Faculty of Sciences, Torino University and INFN - Alessandria, Italy[f]

D.C. Bailey, C.-P. Fagerstroem, R. Galea, G.F. Hartner, K.K. Joo, G.M. Levman, J.F. Martin, R.S. Orr, S. Polenz, A. Sabetfakhri, D. Simmons, R.J. Teuscher[5]
University of Toronto, Department of Physics, Toronto, Ont., Canada[a]

J.M. Butterworth, C.D. Catterall, T.W. Jones, J.B. Lane, R.L. Saunders, M.R. Sutton, M. Wing
University College London, Physics and Astronomy Department , London, UK[o]

J. Ciborowski, G. Grzelak[40], M. Kasprzak, K. Muchorowski[41], R.J. Nowak, J.M. Pawlak, R. Pawlak, T. Tymieniecka, A.K. Wróblewski, J.A. Zakrzewski
Warsaw University, Institute of Experimental Physics, Warsaw, Poland[j]

M. Adamus
Institute for Nuclear Studies, Warsaw, Poland[j]

C. Coldewey, Y. Eisenberg[37], D. Hochman, U. Karshon[37]
Weizmann Institute, Department of Particle Physics, Rehovot, Israel[d]

W.F. Badgett, D. Chapin, R. Cross, S. Dasu, C. Foudas, R.J. Loveless, S. Mattingly, D.D. Reeder, W.H. Smith, A. Vaiciulis, M. Wodarczyk
University of Wisconsin, Department of Physics, Madison, WI, USA[p]

A. Deshpande, S. Dhawan, V.W. Hughes
Yale University, Department of Physics, New Haven, CT, USA[p]

S. Bhadra, W.R. Frisken, M. Khakzad, W.B. Schmidke
York University, Department of Physics, North York, Ont., Canada[a]

Received: 18 November 1997

Abstract. Charged particles ($h^{\pm}$) and K^0 mesons have been studied in photoproduced events containing at least one jet of $E_T > 8\,\mathrm{GeV}$ in a pseudorapidity interval (–0.5, 0.5) in the ZEUS laboratory frame. Distributions are presented in terms of transverse momentum, pseudorapidity and distance of the particle from the axis of a jet. The properties of $h^{\pm}$ within the jet are described well using the standard settings of PYTHIA, but the use of the multiparton interaction option improves the description outside the jets.

A reasonable overall description of the K^0 behaviour is possible with PYTHIA using a reduced value of the strangeness suppression parameter. The numbers of $h^{\pm}$ and K^0 within a jet as defined above are measured to be $3.25 \pm 0.02 \pm 0.28$ and $0.431 \pm 0.013 \pm 0.088$ respectively. Fragmentation functions are presented for $h^{\pm}$ and K^0 in photoproduced jets; agreement is found with calculations of Binnewies et al. and, at higher momenta, with $p\bar{p}$ scattering and with standard PYTHIA. Fragmentation functions in direct photoproduced events are extracted, and at higher momenta give good agreement with data from related processes in e^+e^- annihilation and deep inelastic ep scattering.

1 Introduction

When a high energy photon interacts with a proton, a QCD-governed hard scattering process may take place in which either the photon, or a parton within the photon, interacts with a parton in the proton. A signature for such processes is high-E_T jets in the final state. Both H1 and ZEUS at HERA have reported measurements of various aspects of jet photoproduction [1–5]. In general terms, the properties of particles in jets depend on the type of leading parton generated by the hard process, and on the process

[1] also at IROE Florence, Italy
[2] now at Univ. of Salerno and INFN Napoli, Italy
[3] now at Univ. of Crete, Greece
[4] supported by Worldlab, Lausanne, Switzerland
[5] now at CERN
[6] retired
[7] also at University of Torino and Alexander von Humboldt Fellow at DESY
[8] now at Dongshin University, Naju, Korea
[9] also at DESY
[10] Alfred P. Sloan Foundation Fellow
[11] supported by the Polish State Committee for Scientific Research, grant No. 2P03B14912
[12] supported by an EC fellowship number ERBFMBICT 950172
[13] now at SAP A.G., Walldorf
[14] visitor from Florida State University
[15] now at ALCATEL Mobile Communication GmbH, Stuttgart
[16] supported by European Community Program PRAXIS XXI
[17] now at DESY-Group FDET
[18] now at DESY Computer Center
[19] visitor from Kyungpook National University, Taegu, Korea, partially supported by DESY
[20] now at Fermi National Accelerator Laboratory (FNAL), Batavia, IL, USA
[21] now at NORCOM Infosystems, Hamburg
[22] now at Oxford University, supported by DAAD fellowship HSP II-AUFE III
[23] now at ATLAS Collaboration, Univ. of Munich
[24] on leave from MSU, supported by the GIF, contract I-0444-176.07/95
[25] supported by DAAD, Bonn
[26] now a self-employed consultant
[27] supported by an EC fellowship
[28] PPARC Post-doctoral Fellow
[29] now at Osaka Univ., Osaka, Japan
[30] supported by JSPS Postdoctoral Fellowships for Research Abroad
[31] now at Wayne State University, Detroit
[32] partially supported by Comunidad Autonoma Madrid
[33] partially supported by the Foundation for German-Russian Collaboration DFG-RFBR
(grant no. 436 RUS 113/248/3 and no. 436 RUS 113/248/2)
[34] now at Department of Energy, Washington
[35] supported by the Feodor Lynen Program of the Alexander von Humboldt foundation
[36] Glasstone Fellow
[37] supported by a MINERVA Fellowship
[38] now at ICEPP, Univ. of Tokyo, Tokyo, Japan
[39] present address: Tokyo Metropolitan College of Allied Medical Sciences, Tokyo 116, Japan
[40] supported by the Polish State Committee for Scientific Research, grant No. 2P03B09308
[41] supported by the Polish State Committee for Scientific Research, grant No. 2P03B09208
[a] supported by the Natural Sciences and Engineering Research Council of Canada (NSERC)
[b] supported by the FCAR of Québec, Canada
[c] supported by the German Federal Ministry for Education and Science, Research and Technology (BMBF), under contract numbers 057BN19P, 057FR19P, 057HH19P, 057HH29P, 057SI75I
[d] supported by the MINERVA Gesellschaft für Forschung GmbH, the German Israeli Foundation, and the U.S.-Israel Binational Science Foundation
[e] supported by the German Israeli Foundation, and by the Israel Science Foundation
[f] supported by the Italian National Institute for Nuclear Physics (INFN)
[g] supported by the Japanese Ministry of Education, Science and Culture (the Monbusho) and its grants for Scientific Research
[h] supported by the Korean Ministry of Education and Korea Science and Engineering Foundation
[i] supported by the Netherlands Foundation for Research on Matter (FOM)
[j] supported by the Polish State Committee for Scientific Research, grant No. 115/E-343/SPUB/P03/002/97, 2P03B10512, 2P03B10612, 2P03B14212, 2P03B10412
[k] supported by the Polish State Committee for Scientific Research (grant No. 2P03B08308) and Foundation for Polish-German Collaboration
[l] partially supported by the German Federal Ministry for Education and Science, Research and Technology (BMBF)
[m] supported by the Fund for Fundamental Research of Russian Ministry for Science and Education and by the German Federal Ministry for Education and Science, Research and Technology (BMBF)
[n] supported by the Spanish Ministry of Education and Science through funds provided by CICYT
[o] supported by the Particle Physics and Astronomy Research Council
[p] supported by the US Department of Energy
[q] supported by the US National Science Foundation

known as fragmentation (or hadronisation) by which the colour in the jet is neutralised. The main features of the fragmentation of a given leading parton at a given energy are believed to be universal and independent of the type of initiating process. It is fragmentation, moreover, rather than leading strange or charm quarks, which generates most of the strange particles that occur in jets [6]. At the phenomenological level, a longitudinal fragmentation function $D(z)$ may be used to describe the observed momentum distribution of a chosen type of particle along the jet axis, where z is the fraction of the jet momentum taken by the particle. Experimentally, $D(z)$ functions have so far been obtained mainly from fits to e^+e^- collider data.

In the present analysis, using data taken in ep collisions with the ZEUS detector in 1994, we examine the inclusive properties of charged particles and K^0 mesons produced in association with high-E_T photoproduced jets. This work complements the studies of such particles which have been performed in deep inelastic scattering (DIS) by the ZEUS and H1 collaborations [7-10]. The results are compared with predictions obtained from the PYTHIA Monte Carlo generator, which incorporates the Lund string model of particle fragmentation as implemented in JETSET [11]. As one possible improvement to the standard description, the suggestion is investigated that the particle distributions may be affected by an underlying event structure due to multiparton scattering [12].

Several studies are also made in this analysis to test the universality of fragmentation. In deep inelastic scattering [9,10,13], it has been found that the behaviour of charged particles in the current region of the Breit frame is similar to that found in high energy quark jets in e^+e^- annihilation; however, there are indications [7,8,14] that DIS may give jets with a lower strangeness content than expected from the standard settings of PYTHIA. DELPHI [15] has also reported results with a similar conclusion. We investigate whether this applies also to jets produced using incoming photons that are quasi-real, noting that inclusive cross sections of K^0 in photoproduction found by H1 are broadly consistent with PYTHIA predictions [16]. Comparison is also made with the fragmentation function calculations of Binnewies et al. [17], which are based on fits to the particle content of jets at PEP and LEP [18]. To give a more immediate test of the universality of fragmentation in different types of process, we select a sample of events dominated by the direct photoproduction process (i.e. in which the photon interacts in a pointlike manner). These data allow a comparison with e^+e^- and DIS results without any intermediate model or parameterisation.

The structure of the paper is as follows. After an account of the apparatus, the event selection and the selection of charged tracks, the procedure for reconstructing K^0 mesons is discussed. We describe the Monte Carlo models used in simulating the data, and the more important sources of systematic error. Results are then given on the properties of charged particles and K^0 mesons in photoproduced jets. Finally, we present a study of fragmentation functions for both charged particles and K^0 mesons, extracting results for direct photoproduced events in order to make a general comparison with other types of experiment.

2 Apparatus and running conditions

The data used in the present analysis were collected by the ZEUS detector at HERA. During 1994, HERA collided positrons with energy $E_e = 27.5\,\text{GeV}$ with protons of energy $E_p = 820\,\text{GeV}$, in 153 circulating bunches. Additional unpaired positron (15) and proton (17) bunches enabled monitoring of beam related backgrounds. The data sample used in this analysis corresponds to an integrated luminosity of 2.6 pb^{-1}. The luminosity was measured by means of the positron-proton bremsstrahlung process $ep \to e\gamma p$, using a lead-scintillator calorimeter at $Z = -107$ m[1] which intercepts photons radiated at angles of less than 0.5 mrad with respect to the positron beam direction.

The ZEUS apparatus is described more fully elsewhere [19]. Of particular importance in the present work are the central tracking detector (CTD), the vertex detector (VXD) and the uranium-scintillator calorimeter (CAL).

The CTD [20] is a cylindrical drift chamber situated inside a superconducting magnet coil which provides a 1.43 T field. It consists of 72 cylindrical layers covering the polar angle region $15^\circ < \theta < 164^\circ$ and the radial range 18.2–79.4 cm. The transverse momentum resolution for tracks traversing all CTD layers is $\sigma(p_T)/p_T \approx \sqrt{(0.005p_T)^2 + (0.016)^2}$, with p_T in GeV. The VXD [21] supplied tracking inside the CTD, and consisted of 120 radial cells, each with 12 sense wires covering the radial range 10.6–14.3 cm. The vertex position of a typical multiparticle event is determined from the tracks to an accuracy of typically ± 1 mm in the X, Y plane and ± 4 mm in Z.

The CAL [22] gives an angular coverage of 99.7% of 4π and is divided into three parts (FCAL, BCAL, RCAL), covering the forward (proton direction), central and rear polar angle ranges 2.6°–36.7°, 36.7°–129.1° and 129.1°–176.2°, respectively. Each part consists of towers which are longitudinally subdivided into electromagnetic (EMC) and hadronic (HAC) readout cells. From test beam data, energy resolutions of $\sigma_E/E = 0.18/\sqrt{E}$ for electrons and $\sigma_E/E = 0.35/\sqrt{E}$ for hadrons have been obtained (with E in GeV). The calorimeter cells also provide time measurements which are used for beam-gas background rejection.

3 Trigger and event selection

To identify jets in the event trigger and the subsequent selection of events, a cone algorithm [4] in accordance

[1] The ZEUS coordinates form a right-handed system with positive-Z in the proton beam direction and a horizontal X-axis. The nominal interaction point is at $X = Y = Z = 0$. Pseudorapidity η is defined as $-\ln\tan\theta/2$, where θ is the polar angle relative to the Z direction. In the present analysis, η is always defined in the laboratory frame, and the actual interaction point of the event is taken into account

with the Snowmass Convention [23] was applied to the calorimeter cells. Each cell signal was treated as corresponding to a massless particle. A cone radius of 1.0 in $R = \sqrt{(\delta\phi)^2 + (\delta\eta)^2}$ was used, where $\delta\phi$, $\delta\eta$ denote the distances of cells from the centre of the jet in azimuth and pseudorapidity. A similar algorithm was used both online and offline. The transverse energy of the reconstructed jet is the sum of the measured transverse energies of the calorimeter cells included in it, and will be referred to as E_T^{rec}.

The ZEUS detector uses a three-level trigger system. The first level trigger selected events on the basis of a coincidence of a regional or transverse energy sum in the calorimeter and a track in the CTD pointing towards the interaction point. At the second level, at least 8 GeV of transverse energy was demanded, excluding the eight calorimeter towers surrounding the forward beam pipe. Beam-gas background is further reduced using the measured times of energy deposits and the summed energies in the calorimeter. At the third level, jets were identified. The trigger combination used in the present study required at least one jet with $E_T^{rec} > 6.5$ GeV and $\eta < 2.5$, or with $E_T^{rec} > 5.5$ GeV and $\eta < 2.0$. Cosmic ray events were rejected by means of information from the CTD and the calorimeter. An interaction vertex at a position $Z > -75$ cm, as determined from the CTD tracks, was demanded. A total of 392k events passed these requirements. The trigger efficiency is close to 100% over the entire kinematic range of events used in the present analysis.

To study the association of K_s^0 mesons with jets, it was necessary to obtain a sample of high energy jets sufficiently centred in the acceptance of the CTD so as to optimise the acceptance for the π^+ and the π^- decay products of associated K_s^0 mesons. With these considerations in mind, events were selected offline with at least one jet having $E_T^{rec} > 7$ GeV and $|\eta| < 0.5$. Standard ZEUS background rejection criteria were applied [3,19] to improve the rejection of beam-gas events and cosmic ray events by means of cuts on the primary vertex position, the fraction of well-measured tracks, the CAL signal times and the transverse momentum imbalance in the event. On the assumption that the outgoing positron is not detected in the CAL, $y_{JB} = \sum(E - p_Z)/2E_e$ was calculated, where the sum is over all calorimeter cells, treating each signal as equivalent to a massless particle; i.e. E is the energy deposited in the cell, and p_Z is the value of $E\cos\theta$. The quantity y_{JB} is then a measure of $y^{true} = E_{\gamma,in}/2E_e$, where $E_{\gamma,in}$ is the energy of the incident virtual photon. In the case that a DIS positron is present, a value of approximately unity is obtained. Events containing a DIS positron were rejected by requiring that (i) no scattered beam positron be identified in the CAL, and (ii) $y_{JB} < 0.7$. A requirement of $y_{JB} \geq 0.15$ was also imposed as part of the beam-gas background rejection procedure. After these cuts, the accepted events had photon virtualities of $Q^2 \lesssim 4\,\mathrm{GeV}^2$, with median value $\sim 10^{-3}\,\mathrm{GeV}^2$, and correponded to scattering from partons in the proton with fractional momentum x_p in the approximate range $5\,10^{-3}$–$5\,10^{-2}$. A total of 34.8k events was obtained at this stage, containing 36.6k jets with $E_T^{rec} > 7$ GeV and $|\eta| < 0.5$. This selection of events, each containing at least one accepted jet, represents the basic event sample for the analysis that follows.

4 Charged particle selection

For the study of inclusive charged particle distributions, CTD tracks were accepted if

(1) they were associated with the primary vertex,

(2) their pseudorapidity was in the range $|\eta| \leq 1.5$, and

(3) their transverse momentum satisfied $p_T \geq 0.5$ GeV.

The pseudorapidity and momentum conditions are chosen to be the same as those to be imposed on the K_s^0 mesons. Apart from a small component arising from short-lived particle decays, these conditions provide a sample of well-measured tracks which can be identified with charged hadrons originating from the main interaction. In the following sections, charged particles will be referred to as $h^{\pm}$.

5 K^0 reconstruction

K^0 mesons decay 50% as K_s^0, which have a 68.6% branching ratio into $\pi^+\pi^-$ [24]. K_s^0 mesons were identified by their charged decay mode $K_s^0 \to \pi^+\pi^-$. This decay mode is easily identifiable given the accurate tracking measurements from the CTD, since the mean decay distance, projected on to the $r\phi$ plane, of $2.67 p_T/m_K$ cm ensures a spatial separation of the decay vertex from the primary event vertex for a large number of the K_s^0 produced in the kinematic conditions of the present analysis.

K_s^0 identification starts by selecting pairs of oppositely charged tracks obtained using the standard ZEUS reconstruction algorithms. In order to restrict the track selection to the kinematic region where the tracking was best understood, each track was required to satisfy the conditions $p_T > 150$ MeV and pseudorapidity $|\eta| < 1.75$. More details of the track reconstruction procedure are given in [7]. Starting with the track parameters determined at the point where the track passes nearest to the beamline, and assuming the tracks in this region to be circular in the $r\phi$ plane, candidate secondary vertices were then found by first calculating the intersection points in the $r\phi$ plane of all pairs of oppositely charged tracks in an event. Zero or two such intersection points are found for a given track pair. The Z-coordinates and the momentum components of each track of a pair were then calculated at each of these (r, ϕ) points.

Further selections were made on the kinematic quantities listed below.

(i) *Separation in Z position.* The separation $|\Delta Z|$ of the two tracks at a candidate secondary vertex was required to be less than 3 cm. If a given track pair gave two candidate secondary vertices, the one with smaller $|\Delta Z|$ was chosen.

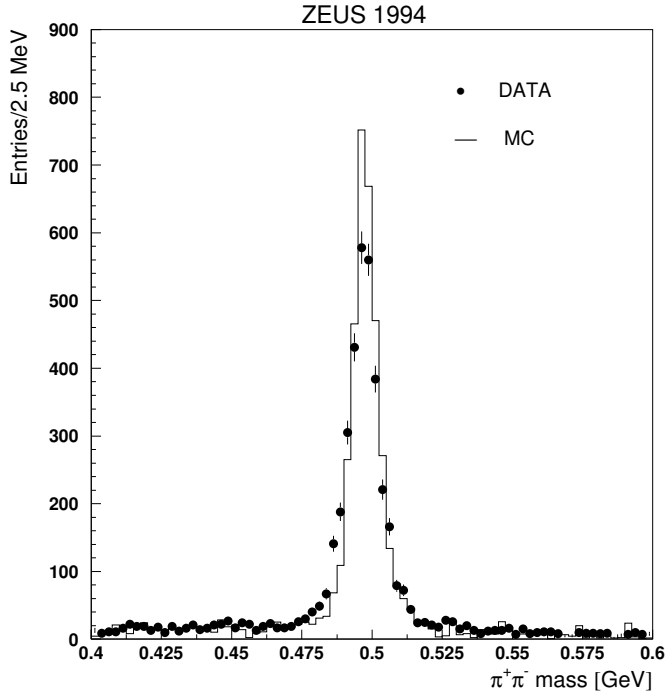

Fig. 1. Reconstructed $\pi^+\pi^-$ mass distribution at selected secondary vertices, compared with Monte Carlo prediction normalized to the total number of events in the plot. The Monte Carlo events show a slightly higher peak/background ratio than in the data

(ii) *Collinearity.* The collinearity angle α is defined as the projected angle in the $r\phi$ plane between the K_s^0 momentum and the line joining the primary to the secondary vertex. Candidates were accepted if $\cos\alpha \geq 0.99$.

(iii) *Track impact parameter.* The impact parameter ϵ of a track is defined as the distance of closest approach between the extrapolated track and the primary event vertex. A requirement $\epsilon > 0.3$ cm was imposed on both tracks for each kaon candidate.

(iv) *Photon conversion.* The effective mass of the two tracks was evaluated assigning zero mass to each track. Track pairs whose effective mass was less than 50 MeV were excluded from further consideration.

(v) *Λ removal.* The $p\pi$ mass hypothesis was applied to each track pair, taking the higher momentum particle to be the p ($\bar{p}$). As in [7], K_s^0 candidates with a $p\pi$ mass less than 1.12 GeV were rejected.

K_s^0 mesons with $p_T \geq 0.5$ GeV and $|\eta| \leq 1.5$ were used in the present analysis. The $\pi^+\pi^-$ mass distribution for all accepted candidates in this kinematic range is shown in Fig. 1, and displays a strong K_s^0 signal. After subtracting a background (averaged over windows between 440–470 and 530–560 MeV) from the signal region of 470–530 MeV, a total of 3154±63 K_s^0 was evaluated on a background of 388. The mean value of the reconstructed K_s^0 mass was 497.0±0.1 MeV (statistical error) compared with the nominal value of 497.7 MeV [24], with a fitted width 6.3±0.1 MeV. Monte Carlo comparisons show that the decay vertex and momentum of the K_s^0 are well reconstructed over the full range of momentum and pseudorapidity, without significant systematic bias. This background subtraction method was used to obtain the K_s^0 signal in each bin of all plotted distributions. The data had a slightly higher background under the mass peak than did the Monte Carlo; this is correctly subtracted out in either case. Further details of the K_s^0 reconstruction may be found in [25].

6 Monte Carlo simulations and data correction

The experimental data were compared with Monte Carlo generated events obtained using PYTHIA 5.7, with JETSET 7.4 for the hadronisation [11]. Systematic studies were made using HERWIG 5.8 [26]. PYTHIA is found to give a reasonable description of jet profiles in hard photoproduction in the kinematic region of the present study [27,28]. PYTHIA events were generated using a $p_{T\,min}$ value of 2.5 GeV as the cut-off for the hard subprocess; the results were insensitive to this choice. The event generation was followed by a full simulation of the detector and trigger response in ZEUS by means of GEANT 3.13 [29]. The direct and resolved contributions are combined in proportion to their generated cross sections. The GRV-LHO parton densities for the photon [30] and MRSA for the proton [31] were used in running the standard version of PYTHIA. Variations on the standard calculation were made by reweighting the results to use different photon parton densities, and also by using an option which uses multiparton interactions (MI) as a model for an underlying event accompanying the main hard QCD subprocess (with a $p_{T\,min}$ value of 1.4 GeV for the secondary interactions). In the LO QCD model employed here, multiparton scattering may accompany the resolved processes, in which the photon acts as a source of partons, but cannot accompany the direct process, in which the photon interacts as a pointlike entity with no partonic substructure.

Within string fragmentation models such as PYTHIA, the most important quantity governing the number of strange particles that appear in the fragmentation is the so-called "strangeness suppression parameter" P_s/P_u. This is assigned a default value of 0.3 on the basis of measurements at PETRA and PEP [32], which measured a variety of strange/non-strange particle ratios (e.g. K^0 to $\pi^\pm$ mesons) in the products of e^+e^- annihilation. In previous studies of neutral kaons in DIS at HERA [7,8] it was found that decreasing P_s/P_u from its standard value improved the agreement between the Monte Carlo and the data. We have therefore generated Monte Carlo event samples also with the value of P_s/P_u decreased from 0.3 to 0.2.

The Monte Carlo events were used to determine correction factors for the data. These were calculated separately for each bin of any given plot, so that for each plotted quantity the corrections are suitably averaged over the other physical quantities. For K^0 calculations, the following factors were taken into account:

(i) *K_s^0 reconstruction efficiency $\epsilon_{K_s^0}$.* Given a set of reconstructed and accepted Monte Carlo events, this was the ratio of (a) the number of reconstructed $K_s^0 \to \pi^+\pi^-$ entries in a given bin, background subtracted, to (b) the corresponding number of generated $K_s^0 \to \pi^+\pi^-$ occurring in this bin. All the other event selection criteria are applied in the normal way.

(ii) *Reconstruction level/hadron level correction factor C.* This factor makes use of jets reconstructed from the four-vectors of the primary final state particles (charged or uncharged) in the generated events, referred to as "hadron jets". For events with a generated $K_s^0 \to \pi^+\pi^-$ in a given bin, C is defined as the ratio of (a) the number of events which satisfy the trigger and acceptance conditions and have a reconstructed calorimeter jet with $E_T^{rec} > 7\,\text{GeV}$ and $|\eta| < 0.5$, to (b) the number of events having $0.2 \le y^{true} < 0.85$ and a hadron jet with cone radius 1.0, $E_T \ge 8\,\text{GeV}$ and $|\eta| \le 0.5$. In this way we correct to a defined set of kinematic conditions at the final state level. The parameters in (b) are chosen to provide a good correspondence with the cuts at the detector level, and thereby minimise the corrections. The y^{true} range corresponds to a γp centre of mass energy range of 134–277 GeV.

Since the shapes of the distributions are similar in the data and Monte Carlo (after reconstruction), the calculated correction factors will suitably take into account all effects due to reconstruction efficiency, event selection efficiency and bin-to-bin migration. These aspects have been checked in our previous studies of inclusive jet production [4]. The K_s^0 reconstruction efficiency is dominated by the geometric effects of the track cuts and the CTD tracking efficiency, with little sensitivity to the properties of the jet. It is similar for direct and resolved events. In the region of p_T and η used here, $\epsilon_{K_s^0}$ has a plateau of approximately 0.35 in the middle of the accepted range of either quantity, falling to 0.25 at the ends. C takes values typically between 0.6 and 0.8.

Corrected numbers of K^0 mesons in bins Δv of any given variable v are evaluated according to the formula

$$\frac{dN(corrected)}{dv} = \frac{N(detected)}{\Delta v\, \epsilon_{tot}\, B}, \qquad (1)$$

where $\epsilon_{tot} = \epsilon_{K_s^0}\, C$, and B is the total branching ratio $K^0 \to K_s^0 \to \pi^+\pi^-$.

For charged particles, a similar relationship $\epsilon_{tot} = \epsilon_{h^\pm}\, C$ is used, where the charged particle reconstruction efficiency $\epsilon_{h^\pm}$ is calculated as the ratio of reconstructed and accepted tracks to the number of generated charged particles in the same bin. C is then calculated analogously to the K^0 case, and B is set to unity. Here and in the calculation of C, generated charged particles are taken to be those in the final state with lifetimes greater than 10^{-8} s, together with charged decay products of primary hadrons with a shorter lifetime than this, but excluding the products of K_s^0 and Λ, $\bar{\Lambda}$ decays.

All the particle distributions are normalised to the number of jets. Keeping in mind that each event in the basic event sample has at least one accepted jet, we evaluate (a) the total number of charged particles or kaons in each bin of a given distribution, and (b) the total number of accepted jets in the basic event sample. The ratio of (a) to (b) is then plotted to give numbers of particles per jet. To obtain corrected distributions, it is thus necessary to correct the total number of measured jets N_{jets}, in the defined kinematic range, to the total number of above-defined hadron jets. To achieve this, the correction formula (1) is again employed, using an efficiency factor $\epsilon_{tot} = C$ together with $B = 1$, and removing from the definition of C the conditions on kaons or charged particles.

7 Systematic uncertainties

The stability of the results against reasonable variations of the selection criteria was studied in order to estimate the systematic uncertainties. The most important effects were estimated as follows:

(1) To study the sensitivity to the fragmentation scheme in the Monte Carlo, HERWIG was used instead of PYTHIA to evaluate the correction factors.

(2) An uncertainty exists in the matching of the calorimeter energy scale in the Monte Carlo events to that of the data. To estimate this, the Monte Carlo energy scale was varied by ±5%.

(3) To estimate tracking uncertainties, the effect of including or not including the VXD in the track reconstruction was investigated.

(4) The effect of varying the accepted y_{JB} range to $0.2 < y_{JB} < 0.8$ was evaluated.

(5) K^0 definition:
(i) the cut on $|\Delta Z|$ was varied between 2 and 4 cm;
(ii) the cut on $\cos\alpha$ was varied by ±0.005;
(iii) the cut on the track impact parameter $|\epsilon|$ was varied in the range 0.27–0.33 cm;
(iv) the upper mass value for Λ rejection was varied between 1.117 and 1.123 GeV.

The effects on the results of most of the parameter variations listed were normally found to be small, at the level of up to a few percent. The individual contributions were combined in quadrature to give the total systematic error on a given point. The systematic errors on the correction factors are dominated by the effects of (1), (2) and (3). The comparison of uncorrected data with PYTHIA predictions is affected by (2) and (3).

8 Results

8.1 Charged particles

In Fig. 2 we present efficiency and acceptance corrected distributions of $dN(h^\pm)/dp_T^2$ and $dN(h^\pm)/d\eta$ in $p_T(h^\pm)$ and $\eta(h^\pm)$ respectively. As defined in Sect. 6, the corrected distributions are given for particles in events containing a final state hadron jet of $E_T(\text{jet}) \ge 8\,\text{GeV}$ with $|\eta(\text{jet})| \le 0.5$. Here and throughout, all results are normalised as

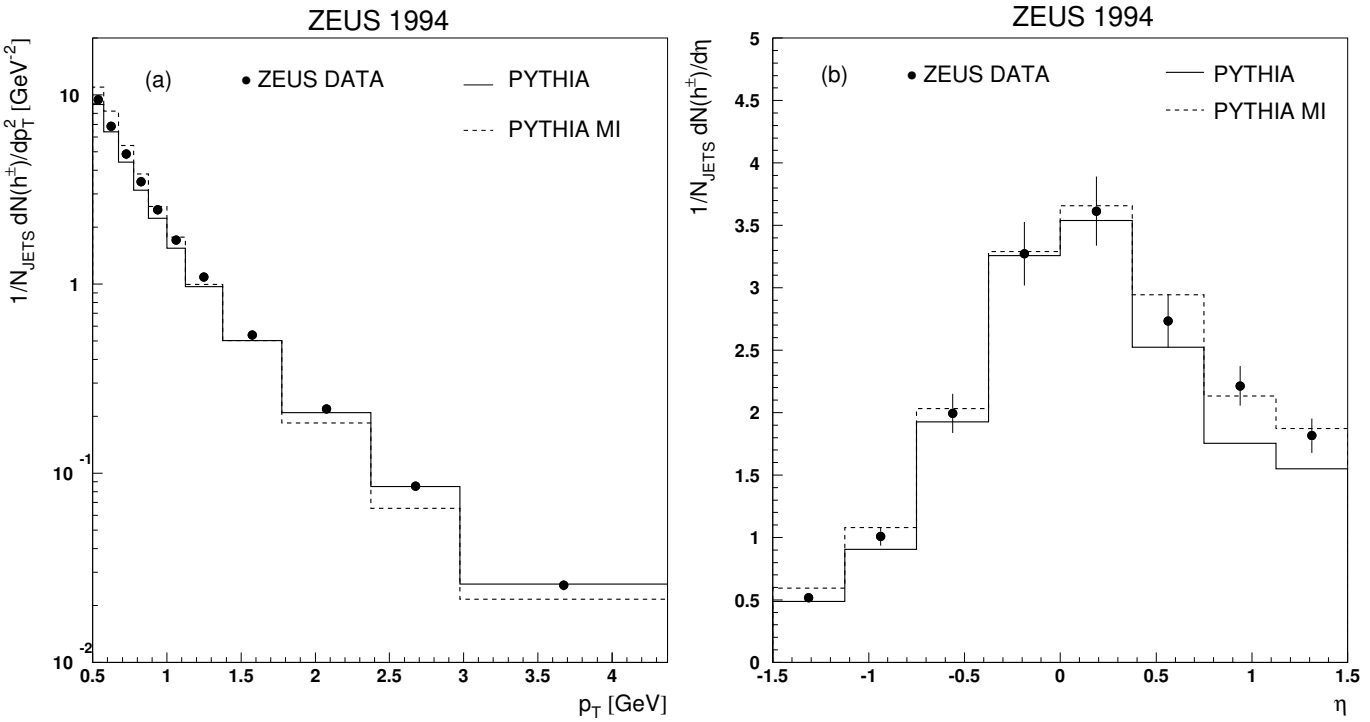

Fig. 2. Corrected distributions of charged particles per jet in events containing a hadron jet with $E_T(\text{jet}) \geq 8\,\text{GeV}$ and $|\eta(\text{jet})| \leq 0.5$. **a** $(1/N_{jets})\, dN(h^{\pm})/dp_T^2$ as a function of $p_T(h^{\pm})$ for $|\eta(h^{\pm})| \leq 1.5$; **b** as a function of $\eta(h^{\pm})$ for $p_T(h^{\pm}) \geq 0.5\,\text{GeV}$. *Error bars* are statistical and systematic combined in quadrature, and are dominated by the systematic. The PYTHIA MI Monte Carlo uses a multiparton interaction model

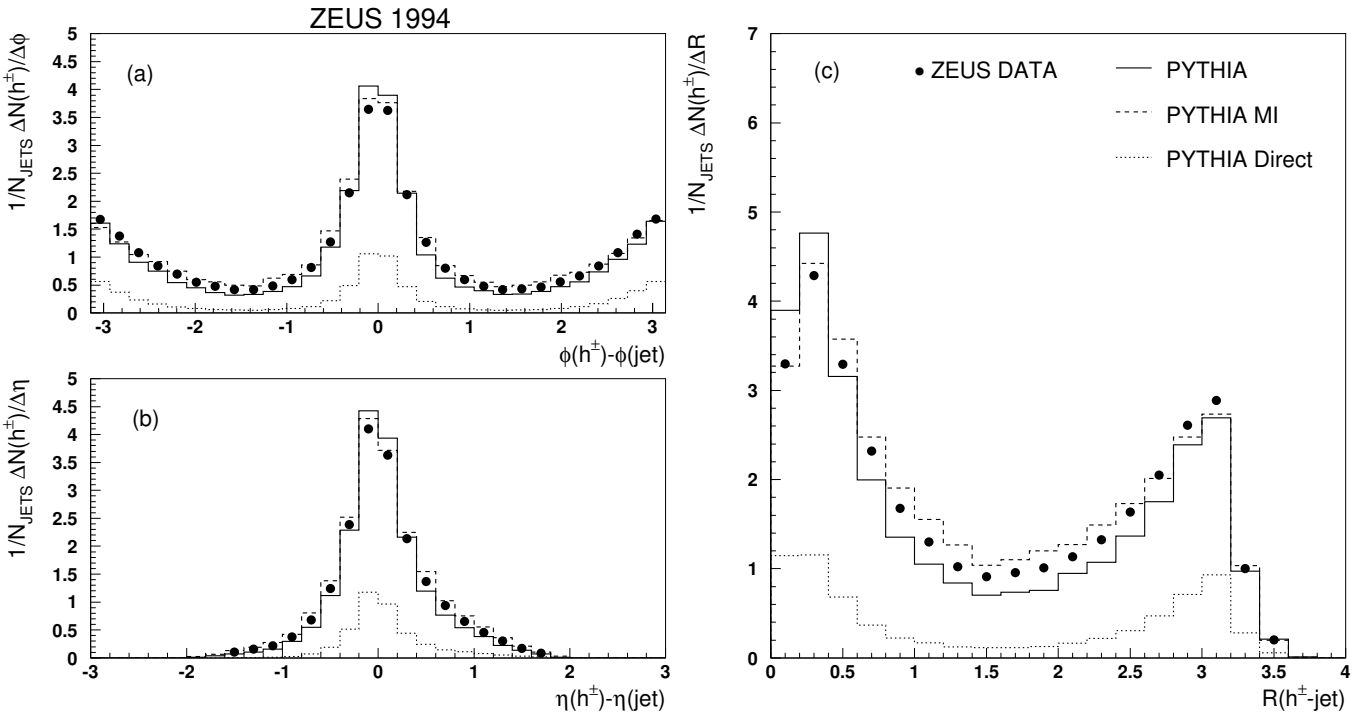

Fig. 3. Distance of charged particles ($h^{\pm}$) from jet **a** in ϕ, **b** in η, for $|\Delta\phi| < \pi/2$, **c** in (η, ϕ), with comparison to various Monte Carlo predictions as indicated. The entries are uncorrected numbers of charged particles ($p_T \geq 0.5\,\text{GeV}$, $|\eta| \leq 1.5$) per measured jet ($E_T^{rec} \geq 7\,\text{GeV}$, $|\eta| \leq 0.5$) per unit interval of the plotted quantity. The *histograms* correspond to PYTHIA predictions using the GRV-LHO photon structure and default strangeness suppression. The direct contribution to the standard PYTHIA calculation is also shown separately. A common systematic error of 5% should be allowed on the data points in comparing with the Monte Carlo

numbers of particles per jet satisfying the stated definitions. The $p_T(h^\pm)$ distributions are averaged over $-1.5 \leq \eta(h^\pm) < 1.5$; the $\eta(h^\pm)$ distributions are averaged over $p_T(h^\pm) \geq 0.5\,\text{GeV}$. At this stage no explicit association of the $h^\pm$ with the jets is made. The statistical errors are small.

Good agreement is seen between the data and the standard PYTHIA predictions in the shape and magnitude of the p_T distribution. In the η distribution, the overall agreement is still good, but it is apparent that standard PYTHIA tends to undershoot the data at higher η values. A similar trend has been observed in other photoproduction studies at HERA [2,4,27], leading to suggestions that the discrepancy can be attributed at least in part to multiparton interactions [12]. The MI option is seen to give an improved description of the data at high η; however, it overestimates the exponential slope of the p_T distribution. A reduction in the P_s/P_u value has a negligible effect on the present distributions (not shown). Little difference is seen if different photon parton densities are used.

We now examine in more detail the association of charged particles with jets, given the presence of at least one jet in each event in the selected data sample. Figure 3a shows the uncorrected distribution in the difference $\Delta\phi$ in azimuth between an $h^\pm$ and the axis of any jet in the event satisfying $E_T^{rec} \geq 7\,\text{GeV}$ and $|\eta(\text{jet})| \leq 0.5$. The peak around $|\Delta\phi| = \pi$ indicates the presence of jets opposite in azimuth to the observed particle. For $h^\pm$-jet pairs with $|\Delta\phi| < \pi/2$, the distance $\Delta\eta$ in pseudorapidity between the $h^\pm$ and the jet is plotted in Fig. 3b. In comparing the data to the Monte Carlo predictions, an overall systematic uncertainty of $\pm 5\%$ should be allowed.

In discriminating between the various models, a particularly useful variable was found to be $R = \sqrt{(\Delta\phi)^2 + (\Delta\eta)^2}$, i.e. the distance in (η, ϕ) between a given particle and the jet axis. The uncorrected R distribution is presented in Fig. 3c. A prominent peak at small R demonstrates that the $h^\pm$ are being produced in association with jets; there is also a peak at $R \approx 3$ due to the likely existence of another jet opposite in ϕ to the first. In the following discussion we concentrate mainly on the region $R < 2.5$. Over the whole range, the main contributions come from resolved processes. The predictions of standard PYTHIA lie slightly above the data at low R, but are low in the inter-jet region $1 < R < 2.5$. To establish whether the latter discrepancy is associated with the excess of $h^\pm$ over expectations seen at high $\eta(h^\pm)$ a similar plot was made with the $h^\pm$ acceptance changed to $-1.5 < \eta(h^\pm) < 0.5$ (not shown). This reduced the discrepancy for $1 < R < 2.5$ slightly but did not eliminate it. Variations of the P_s/P_u parameter and the photon parton density again have little effect on the distributions. The effect of using the MI option of PYTHIA is more pronounced; in the inter-jet region, the MI option overcompensates for the previous shortfall of standard PYTHIA events, while at small R the jet appears broadened. Overall, the MI option provides an improved description of the data.

The mean corrected multiplicity of charged particles with $p_T(h^\pm) \geq 0.5\,\text{GeV}$ per jet, integrated over $R \leq 1$, is shown in Table 1 compared with different results from PYTHIA. All the models are consistent with the experimental result, within errors.

8.2 K^0 mesons

In the previous section it was seen that the features of charged particles in photoproduced jets are generally well described using standard PYTHIA, with some further improvement obtainable using the MI option. Turning now to K^0 mesons, we consider the same distributions as for the $h^\pm$. As before, at least one reconstructed calorimeter jet with $E_T^{rec} \geq 7\,\text{GeV}$ and $|\eta(\text{jet})| \leq 0.5$ was demanded in an event, and the corrected distributions are for events containing a final-state hadron jet with $E_T(\text{jet}) \geq 8\,\text{GeV}$ and $|\eta(\text{jet})| \leq 0.5$. The distributions are normalised as numbers of K_s^0 or K^0 per jet for uncorrected or corrected data respectively. Corrected $dN(K^0)/dp_T^2$ and $dN(K^0)/d\eta$ distributions are shown in Fig. 4 as functions of $p_T(K^0)$ and $\eta(K^0)$. The $p_T(K^0)$ distributions are averaged over $-1.5 < \eta(K^0) < 1.5$; the $\eta(K^0)$ distributions are averaged over $p_T(K^0) \geq 0.5\,\text{GeV}$. No attempt is yet made to associate the K_s^0 with jets. In the larger error bars the systematic and statistical errors are summed in quadrature. Following the studies mentioned [7,8], we also show results with the value of P_s/P_u decreased from 0.3 to 0.2.

A reasonable overall agreement is seen between the data and the various PYTHIA plots in the shape and magnitude of the p_T spectrum, although the MI option tends to overestimate the slope of the plot. For $\eta(K^0) \leq 0.5$, the data of Fig. 4b show an approximate agreement with the standard PYTHIA which is improved by using a reduced value of P_s/P_u. At higher $\eta(K^0)$, however, a tendency for the PYTHIA values to be low compared with the data is worsened when P_s/P_u is reduced. The agreement in this region is improved with the use of the MI option.

Figure 5a shows the uncorrected distribution in the difference $\Delta\phi$ in azimuth between a K_s^0 and any jet in the event satisfying $E_T^{rec} > 7\,\text{GeV}$ and $|\eta(\text{jet})| \leq 0.5$. For K_s^0-jet pairs with $|\Delta\phi| < \pi/2$, the distance $\Delta\eta$ in pseudorapidity between the K_s^0 and the jet is plotted in Fig. 5b. A common overall systematic uncertainty of $\pm 7\%$ should be allowed. The data are reasonably well fitted by the Monte Carlo outside the peak at $\Delta\phi \approx 0$ and in the wings of the $\eta(K^0)$ distribution. In both distributions, standard PYTHIA overestimates the numbers of kaons near the axis of a jet.

The uncorrected distribution in R is plotted in Fig. 5c for all K_s^0. Here it is clear that standard PYTHIA overestimates the data in the jet core, i.e. for $R < 0.4$, while underestimating it in the interjet region. To gain understanding of the possible reasons for the discrepancy in the jet core, a variety of investigations were made. It was found that the discrepancy persists when the number of charged tracks in the region of the jet (i.e. with $R < 1$) is selected to be small: even with just one or two charged particles present in addition to the K_s^0, a similar effect is

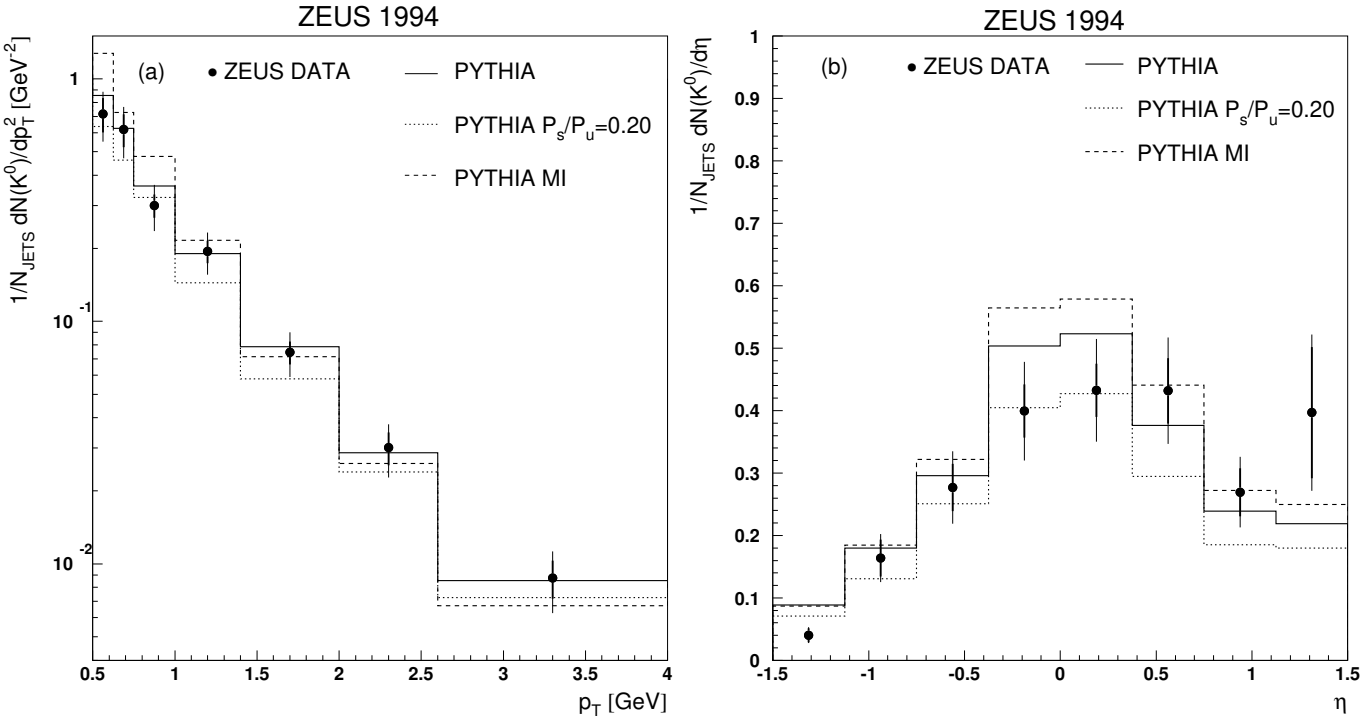

Fig. 4. Corrected distributions of K^0 mesons per jet in events containing a hadron jet with $E_T(\text{jet}) \geq 8\,\text{GeV}$ and $|\eta(\text{jet})| \leq 0.5$. **a** $(1/N_{jets})\,dN(K^0)/dp_T^2$ as a function of $p_T(K^0)$ for $|\eta(K^0)| \leq 1.5$; **b** $(1/N_{jets})\,dN(K^0)/d\eta$ as a function of $\eta(K^0)$ for $p_T(K^0) \geq 0.5\,\text{GeV}$. *Inner* and *outer error bars* are statistical errors and statistical combined with systematic in quadrature

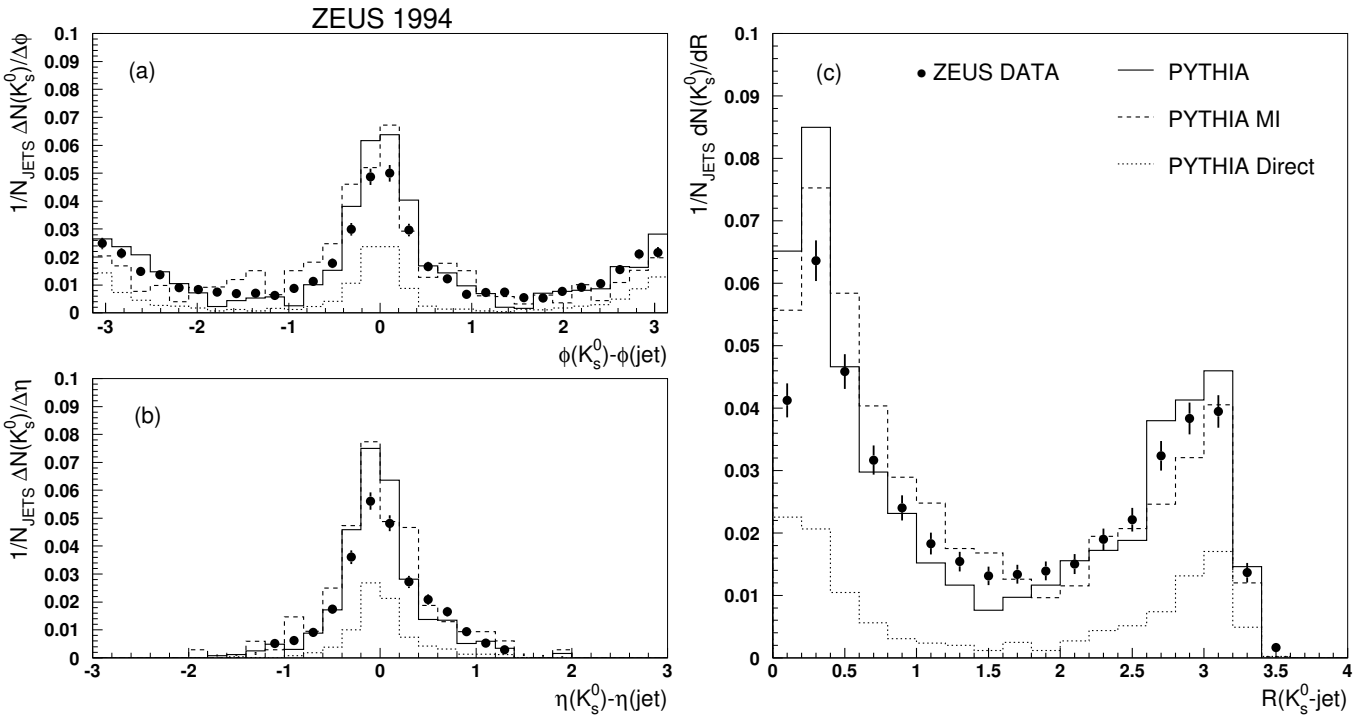

Fig. 5. Distance of K_s^0 from jet **a** in ϕ, **b** in η, for $|\Delta\phi| < \pi/2$, **c** in (η, ϕ), with comparison to various Monte Carlo predictions as indicated. The entries are uncorrected numbers of K_s^0 ($p_T \geq 0.5\,\text{GeV}$, $|\eta| \leq 1.5$.) per measured jet ($E_T^{rec} \geq 7\,\text{GeV}$, $|\eta| \leq 0.5$) per unit interval of the plotted quantity. The *histograms* correspond to PYTHIA predictions using the GRV-LHO photon structure and default strangeness suppression. The direct contribution to the standard PYTHIA calculation is also shown separately. A common systematic error of 7% should be allowed on the data points in comparing with the Monte Carlo

Table 1. Corrected multiplicities of charged particles ($h^{\pm}$) and neutral K^0 mesons ($p_T \geq 0.5\,\text{GeV}$) per photoproduced jet ($E_T(\text{jet}) > 8\,\text{GeV}$, $|\eta(\text{jet})| < 0.5$), cone radius = 1, for $134 < W < 277\,\text{GeV}$. Comparison is made between ZEUS data and PYTHIA Monte Carlo predictions with strangeness suppression parameter $(P_s/P_u) = 0.3$ (standard value) and 0.2, without and with the multiparton interactions (MI) option. The first error quoted is in each case statistical, the second error on the data is systematic.

	DATA	PYTHIA Monte Carlo			
	(ZEUS 1994)	Standard	MI	Standard	MI
P_s/P_u		0.3	0.3	0.2	0.2
$h^{\pm}$	3.25±0.02±0.28	3.31±0.03	3.44±0.06	3.37±0.04	3.46±0.04
K^0	0.431±0.013±0.088	0.513±0.013	0.560±0.025	0.416±0.014	0.426±0.013

seen. In the events used in this analysis, the mean number of additional charged particles in the jet is approximately 3. It is therefore difficult to attribute the effect to a poorly understood problem with the charged particle tracking.

The effects of varying the photon parton densities were investigated and found to be small: the use of the GRV-LO [30], ACFGP [33], LAC1 [34] or GS-HO [35] parton sets altered the predictions by less than 5% for $R < 1$. No attempt was made to vary the parton densities in the proton, since these are well defined in the present kinematic range from other measurements. Removing the small contribution from charm-containing jets in the generated events made only a slight difference, giving little scope for remedying the problem by remodelling the charm simulation. If the normalisation is performed to luminosity rather than to numbers of jets, the conclusions are likewise unchanged. A similar although less marked discrepancy at low R was found using predictions from the HERWIG Monte Carlo. The discrepancy outside the jet is again found to be reduced slightly but not eliminated if the acceptance is reduced to $-1.5 < \eta(K_s^0) < 0.5$. The MI option gives an improved description in the inter-jet region, but is worse elsewhere.

In about 7% of the kaonic events, two K_s^0 were found. The distance R in (η, ϕ) between them was plotted, giving a distribution which was fairly flat up to $R \approx 3.5$ with a small enhancement at low R. Standard PYTHIA tends to overestimate the data by approximately the same amount as at $R < 0.4$ in Fig. 5c, but over the entire R range. The conclusion is that many of the K^0 pairs are not strongly correlated.

The characteristics of the K_s^0 in jets can be further investigated by distinguishing between direct and resolved photoproduction processes, as defined at leading order in QCD. A subsample of events was chosen in which at least two jets were found, one satisfying the above experimental jet definition and a second having $E_T^{rec} > 7\,\text{GeV}$ as before, and $\eta(\text{jet}) < 2.5$. The two highest E_T jets satisfying these conditions were used to estimate the fraction of the photon energy which takes part in the hard subprocess. This estimate is given in terms of the measured parameters of the two jets as $x_\gamma^{\text{OBS}} = (E_{T\,1}^{rec} e^{-\eta_1} + E_{T\,2}^{rec} e^{-\eta_2})/2E_e\, y_{JB}$. For $x_\gamma^{\text{OBS}} < 0.75$ the event samples are dominated by the resolved process, above this value the direct process is more important [27].

In Figs. 6a, 7a, R distributions for the resolved-enhanced and direct-enhanced data samples ($x_\gamma^{\text{OBS}} < 0.75$, $x_\gamma^{\text{OBS}} > 0.75$) are shown, and compared with PYTHIA predictions. A small admixture of generated direct events is found in the PYTHIA samples with $x_\gamma^{\text{OBS}} < 0.75$, and a relatively larger admixture of generated resolved events in the samples with $x_\gamma^{\text{OBS}} > 0.75$. In the inter-jet region, a deficit in the standard PYTHIA predictions is seen in the resolved-enhanced sample but not in the direct-enhanced sample, suggesting the possibility of an association with multiparton interactions. In the jet core, the resolved-enhanced sample shows a much larger discrepancy between the data and standard PYTHIA than does the direct-enhanced sample. The statistical errors on the PYTHIA histograms are similar to those on the data.

In Fig. 6b, we consider the effects of the reduced P_s/P_u value and the MI option in PYTHIA on the resolved-enhanced event sample. The use of the MI option is manifestly advantageous, and is in fact essential in order to obtain reasonable agreement with the data when using $P_s/P_u = 0.2$. A P_s/P_u value between 0.2 and 0.3 appears preferred. While not perfect, the agreement using $P_s/P_u = 0.2$ together with the MI option represents a significant improvement on the standard version of PYTHIA. Similar conclusions emerge from the direct-enhanced sample (Fig. 7) in which, overall, the reduced P_s/P_u value significantly improves the match with the data in the R distribution. The MI option, affecting only the resolved contribution to the histograms, has a positive effect. A P_s/P_u value intermediate between 0.2 and 0.3 might represent a further improvement.

The mean corrected multiplicity of K^0 with $p_T(K^0) \geq 0.5\,\text{GeV}$ per jet, integrated over $R \leq 1$, is shown in Table 1. The full event sample containing one or more jets per event is used. A comparison with the different results from PYTHIA confirms the preference for a lower strangeness suppression parameter in describing the overall numbers of K^0 within the jets.

8.3 Fragmentation functions

In the previous sections, angular distributions of charged particles and K_s^0 relative to jets were studied, averaged over the particle momenta. The momentum distributions of particles within a jet may be described by fragmentation

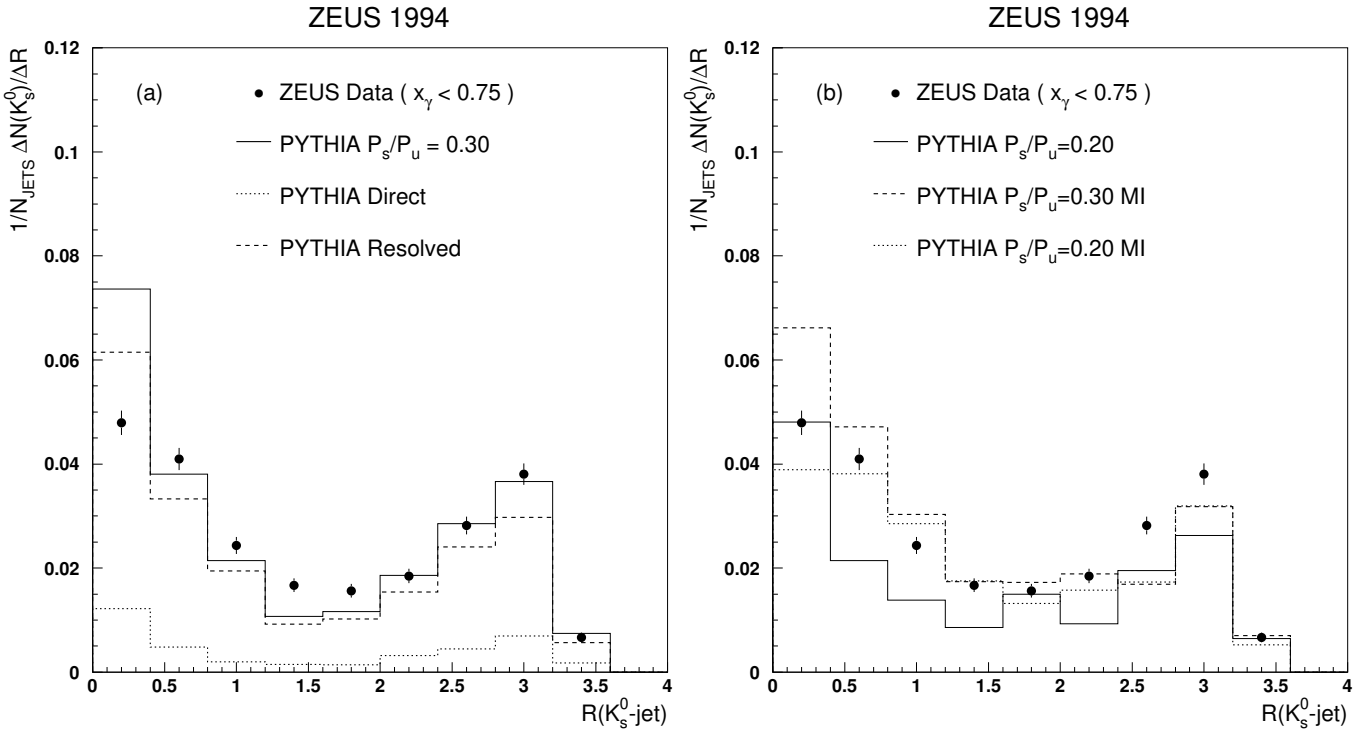

Fig. 6. Uncorrected R distributions for resolved-enhanced events ($x_\gamma^{\rm OBS} < 0.75$) compared **a** with standard version of PYTHIA ($P_s/P_u = 0.3$), showing also the direct and resolved contributions separately, **b** with PYTHIA using $P_s/P_u = 0.2$, MI option, and both variants together. Kinematic definitions are as in Fig. 5

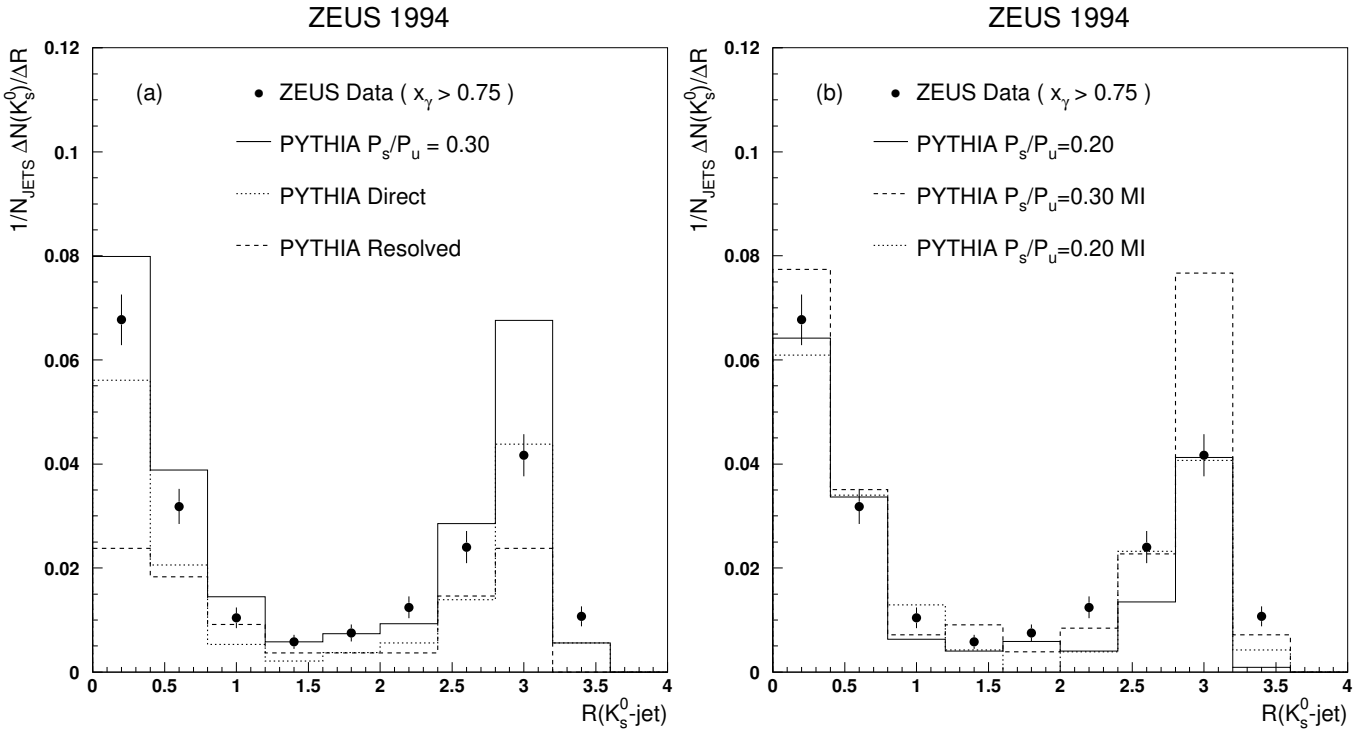

Fig. 7. Uncorrected R distributions for direct-enhanced events ($x_\gamma^{\rm OBS} > 0.75$) compared **a** with standard version of PYTHIA ($P_s/P_u = 0.3$), showing also the direct and resolved contributions separately, **b** with PYTHIA using $P_s/P_u = 0.2$, MI option, and both variants together. Kinematic definitions are as in Fig. 5

functions $D(z)$, where z is a measure of the fraction of the jet momentum taken by the particle. $D(z)$ is defined as $(1/N_{jets})\, dN(X)/dz$, where X denotes a charged particle or K^0. A particle is defined here as being associated with a given jet if it satisfies the criterion $R < 1$.

The variable z may be defined in several ways. In the usage of CDF [36], the longitudinal component of the particle momentum along the jet axis is scaled by the jet energy according to a formula which may be written as $z_L = \mathbf{p}(X) \cdot \mathbf{n}(\text{jet})/E(\text{jet})$. Here $\mathbf{p}$ denotes the momentum 3-vector of a particle, and $\mathbf{n}$(jet) is a unit vector along the jet axis. An alternative approach is to take the energy ratio $z_E = E(X)/E(\text{jet})$. This is analogous to the definition $z = E(X)/E(\text{beam})$ normally used in e^+e^- collider experiments, where E(beam) corresponds to the maximum possible energy E(max) of a leading parton. One notes that in the latter measurements, since they are carried out in the e^+e^- centre of mass frame, the calculated value of z does not depend on the actual production angle of the final state particle, and so is independent of many details of the hadronisation mechanism and higher order effects. No explicit identification of jets is required, or association of particles with jets.

Here we present our results using both definitions of z. The numbers of $h^\pm$, K^0 and jets were corrected as described in Sect. 6. A small systematic overestimate of the z scale at low values exists due to losses of low momentum particles from the reconstructed jet. The loss of energy in dead material in front of the CAL also has the effect of increasing the measured z value. A correction is applied to remove these effects. Results are plotted at the mean z value of the events in a series of chosen z intervals. Values of z_E are typically 10–20% larger on average than those of z_L.

Figures 8a and 9a show the resulting $D(z_L)$ distributions for $h^\pm$ and K^0 respectively, with pion masses assigned to the $h^\pm$. Also plotted are values of the corresponding distribution obtained using PYTHIA. The distributions are averaged over η(jet) and E_T(jet) within the same selected ranges as above. For $z_L < 0.05$ the effects of the 0.5 GeV cut-off on p_T in the $h^\pm$ and K^0 data become important. Good agreement is seen between the data and the standard PYTHIA distributions, in the K^0 case for z_L values above 0.15; in this range it is not possible to discriminate between P_s/P_u values of 0.3 and 0.2. The discrepancy noted in the K^0_s R plots appears to be concentrated at $z_L < 0.15$, where the bulk of the statistics lie, apart from the two highest z_L points with large errors. The MI is in agreement with the $h^\pm$ data at low momenta now that the association of particles with jets has been made. Also shown in Fig. 8a are $D(z_L)$ values from CDF [36], for $h^\pm$ in jets of energy ≈40–100 GeV produced in $p\bar{p}$ scattering. Although the CDF energies are considerably higher than those of the present measurements, and the mixture of leading final state partons is also likely to be different, there is a clear similarity of the fragmentation functions in the range $0.15 < z_L < 0.7$.

For a comparison with e^+e^- data, results from the present measurements are first compared with calculations from the next-to-leading order phenomenological fits of Binnewies et al [17] (Figs. 8b, 9b). These authors have made use of a variety of e^+e^- data sets at different energies to extract separate fragmentation functions for the different types of primary parton in the range $0.1 < z < 0.8$. The approach is based on the different quark couplings to photons and to Z bosons, and on topological properties of events with hard gluon emission. A definition $z = E(X)/E(\text{beam})$ is used; we therefore adopt here the corresponding definition $z = z_E = E(X)/E(\text{jet})$. Since the primary partons in the photoproduced jets are unidentified, and we currently lack a full NLO Monte Carlo simulation of the γp process, a shaded region is drawn to cover the spread of the calculated $D(z)$ values for the fragmentation of gluons and different types of quark (i.e. u, d, s, c). The calculation has been performed using a QCD scale of 8 GeV, corresponding approximately to the present jet E_T values. Details of which parton fragmentation functions contribute to the upper and lower bounds of the shaded regions are given in the figure captions.

Good agreement with the calculations is found, to within their uncertainty as applied to the present data. A few remarks need to be held in mind:

(i) Reference [17] includes charged decay products of long-lived primaries such as K^0_s, Λ in the definition of a charged particle. This gives ≈ 10% more charged hadrons compared with the present method.

(ii) As stated above, a jet definition, and the requirement that the given particle be associated with a jet, are required in our present approach, but not in the e^+e^- based analyses. This tends to lower the distributions in particular at lower z_E values.

(iii) The experimental z_E (or z_L) value is corrected relative to the energy of hadron jets. A correction to the energy of the the final-state leading parton in the hard process has not been attempted here.

More precise comparisons are available using the direct photoproduction process, since a close similarity is expected in general between event properties in direct hard photoproduction, e^+e^- annihilation, and DIS at low x, where x is the Bjorken variable. At energies comparable to those of the present data, e^+e^- annihilation is governed by a single electromagnetic vertex, summed over the different types of quark, while the LO direct photoproduction process is dominated by photon gluon fusion, whose diagrams feature a similar electromagnetic vertex accompanied by a quark-gluon vertex which does not depend on the quark type. In a similar way, in DIS events at low x, the virtual photon couples to quarks that come predominantly from the sea, having evolved through $gq\bar{q}$ vertices which are likewise flavour independent.

We therefore make a comparison between fragmentation functions obtained from the direct photoproduction process in ZEUS, and values obtained from e^+e^- and DIS measurements. Figures 10, 11 show results obtained from the present direct-enhanced event samples, corrected by means of PYTHIA on a bin-by-bin basis to remove the resolved component so as to be equivalent to results from "pure direct" event samples. The correction factors lay in

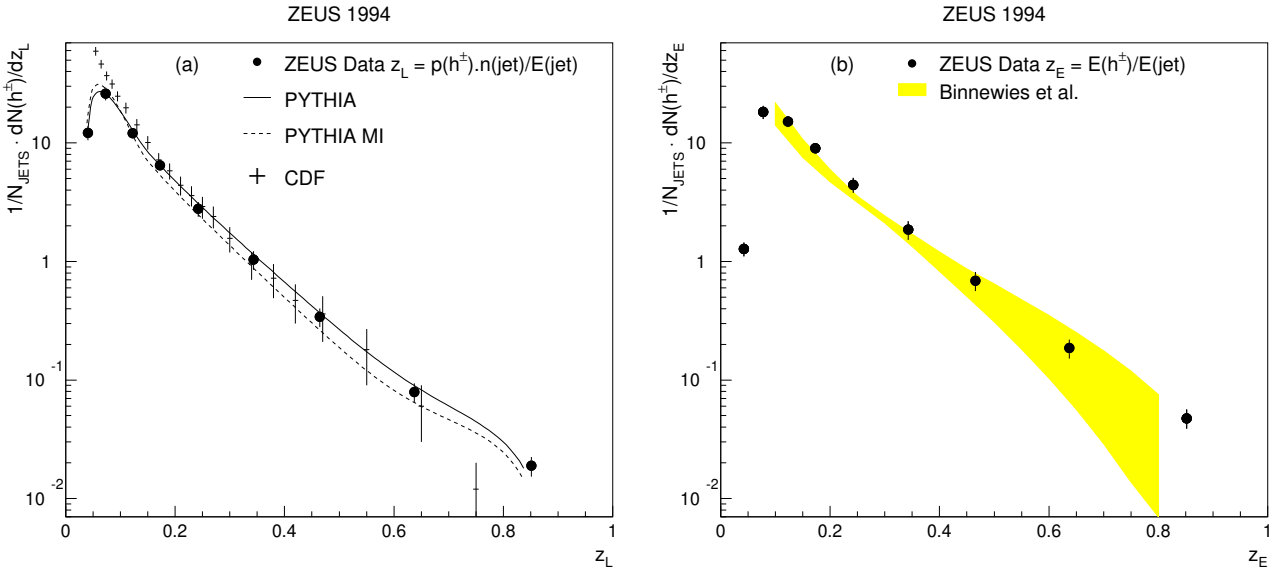

Fig. 8. Corrected fragmentation functions $D(z)$ for charged particles ($h^{\pm}$) with $p_T(h^{\pm}) \geq 0.5\,\text{GeV}$, in hadron jets with $E_T(\text{jet}) > 8\,\text{GeV}$ and $|\eta(\text{jet})| \leq 0.5$; systematic errors dominate. In **a** comparisons are made with variations on the standard version of PYTHIA, and with CDF results in the approximate jet energy range 40–100 GeV; the dominant systematic errors are shown. In **b** the data are compared with a shaded region denoting upper and lower bounds from the phenomenological fit of [17]. The upper bound corresponds to the fitted $D(z)$ values for s, d, u quarks, respectively, in the intervals z = 0.1–0.25, 0.25–0.45, 0.45–0.8. The lower bound corresponds similarly to u, c quarks in the intervals z = 0.1–0.35, 0.35–0.8, respectively

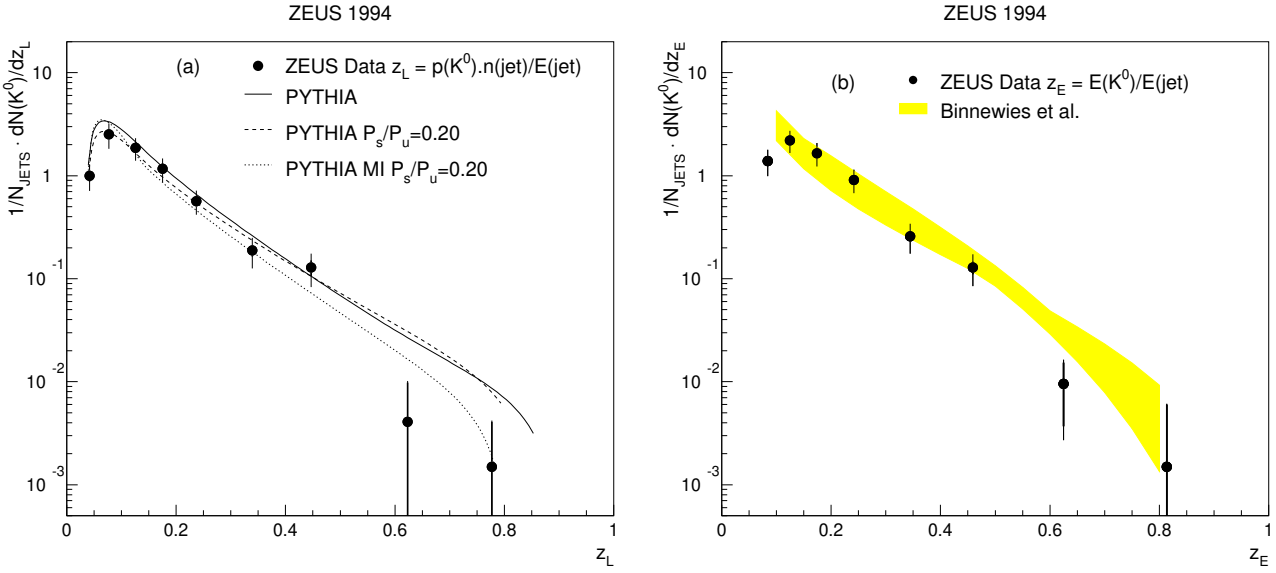

Fig. 9. Corrected fragmentation functions $D(z)$ for K^0. Details as for previous figure. The upper bound of the *shaded region* in **b** corresponds to fitted $D(z)$ values from [17] for $d(=s)$, c, u quarks in the intervals z = 0.1–0.2, 0.2–0.45, 0.45–0.8, respectively. The lower bound corresponds to g, $d(=s)$ in the intervals z = 0.1–0.45, 0.45–0.8, respectively. *Thick error bars* denote dominant statistical errors, *thin* denote dominant systematic errors

the range 0.7–1.1. These are compared with predictions from PYTHIA, and with e^+e^- measurements at similar centre of mass energies to those of the present hard subprocess, i.e. twice the transverse energy of the selected jets. A factor of 0.5 is applied to the published e^+e^- data to allow for the dominant $q\bar{q}$ final state.

For the $h^{\pm}$ data, a further comparison is made to fragmentation functions from ZEUS calculated in the current region of the Breit frame in deep inelastic scattering [10]. Here, data points are used covering a photon virtuality range of $160 < Q^2 < 320\,\text{GeV}^2$ with $0.0024 < x < 0.01$. The corresponding jet energy is $Q/2$, i.e. 6.3–8.9 GeV, roughly equivalent to the jets of the present events. It should be noted that the TASSO data [37] include all charged products from K^0_s and Λ decays, while the ZEUS DIS and ZEUS 1994 photoproduction data exclude all

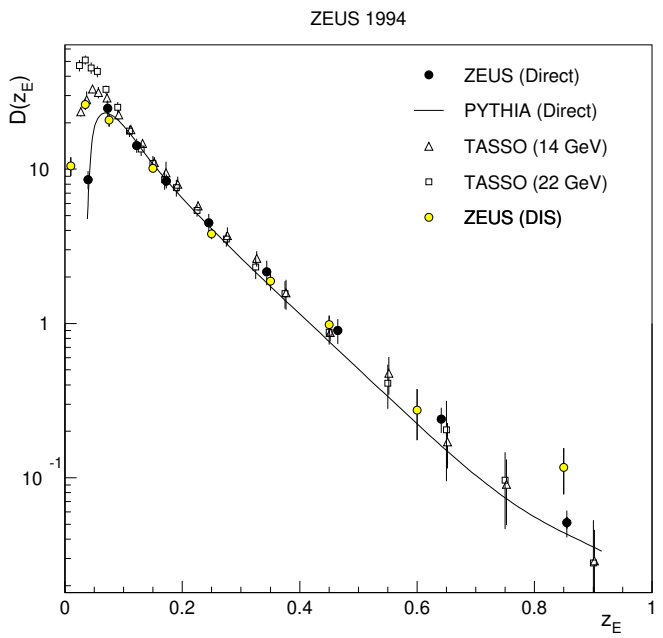

Fig. 10. Fragmentation functions $D(z_E)$ for $h^{\pm}$, obtained from direct-enhanced events and corrected to "pure direct" values. Also plotted are (i) standard PYTHIA predictions for the LO direct process, (ii) data from e^+e^- annihilation at similar jet energies with centre of mass energies as indicated [37], halved to take account of the dominant $q\bar{q}$ final state, and (iii) data from ZEUS measured in deep inelastic scattering [10] with Breit frame jet energies in the range 6.3–8.9 GeV. The variable z_E is defined as $E(h^{\pm})/E(\text{jet})$ for ZEUS 1994 photoproduction data and $z_E = E(h^{\pm})/E(\text{max})$ for the other experimental points. Statistical and total errors on the ZEUS 1994 data are shown as for previous figures; errors are total errors for the TASSO and ZEUS DIS points

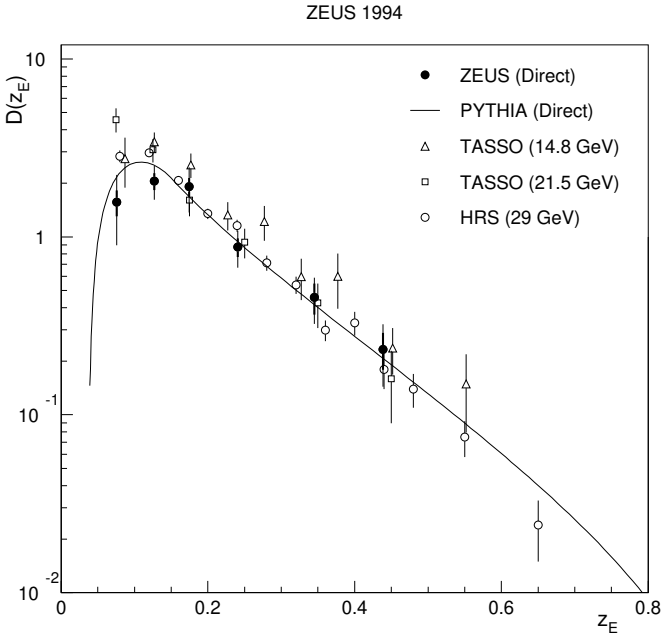

Fig. 11. Fragmentation functions $D(z_E)$ for K^0, obtained from direct-enhanced events and corrected to "pure direct" values; z_E definitions correspond to those for $h^{\pm}$. Also plotted are standard PYTHIA predictions for the LO direct process and data from previous experiments at similar jet energies, with centre of mass energies as indicated [39,40]. Errors on the TASSO and HRS points are total errors

such products; these effects contribute at the level of ±10%. The $h^{\pm}$ data compare well also with pp data from the ISR (not shown) [38] although a different parton mixture is expected in the final state here. For the inclusive K^0 data of [39,40] at different fixed centre of mass energies, the authors quote scaling cross sections which have been converted to fragmentation functions to compare with the present data.

At low z_E, the distributions may be affected by differences between the colour flows in the different types of event, as well as by the cut-off imposed at 0.5 GeV in p_T in the present $h^{\pm}$ and K^0 data, making comparisons between the different data sets difficult. However for $z_E > 0.1$ for $h^{\pm}$, and $z_E > 0.15$ for K^0, the present results are in good agreement with the standard PYTHIA predictions, and the $D(z_E)$ values from the different measurements are also in good agreement with each other. This well illustrates the universality that is believed to be a property of the quark fragmentation process.

9 Summary and conclusions

We have studied the properties of charged particles ($h^{\pm}$) and K^0 mesons in photoproduced events in the ZEUS detector at HERA. The K^0 mesons were studied in the $K^0_s \to \pi^+\pi^-$ decay mode. In each event at least one reconstructed jet was required in the calorimeter with measured $E_T^{rec} > 7$ GeV, centrally produced in the laboratory frame. The distributions of the $h^{\pm}$ and K^0 in these events were studied as a function of a number of kinematic variables; the distance R in (η, ϕ) of the particle from the axis of a jet displayed information which was not so clearly evident from the other distributions.

Correction factors were applied to evaluate the numbers of $h^{\pm}$ and K^0 per jet at the final state hadron level, with $E_T(\text{jet}) > 8$ GeV and $|\eta(\text{jet})| < 0.5$, for events in the γp centre of mass energy range $134 < W < 277$ GeV. Corrected distributions in transverse momentum p_T and pseudorapidity η are given. The corrected numbers of $h^{\pm}$ and K^0 within a jet are evaluated, with a particle defined as being inside a jet if it is within unit radius of the jet axis in (η, ϕ). Fragmentation functions $D(z)$ for $h^{\pm}$ and K^0 in photoproduced jets have also been determined. In comparing the present results with those from theory and from other experiments, two definitions of z are employed, in which the longitudinal momentum component of the particle along the jet axis is scaled to the jet energy (z_L), or the particle energy is similarly scaled (z_E).

The distribution of $h^{\pm}$ within photoproduced jets is found to be fairly well described by the standard version

of PYTHIA, whereas that of K^0 mesons is not. Outside the jets, more $h^{\pm}$ and K^0 are found than predicted; the latter situation can be to some extent remedied by using a version of PYTHIA which includes a simulation of multiparton interactions in resolved events. Taken overall, the numbers of K^0 within the jets correspond to a reduced value of the strangeness suppression parameter P_s/P_u in PYTHIA. When the data are divided into samples enriched in the resolved and direct photoproduction processes respectively, this statement remains true in either case. However the effect is concentrated at z values below ≈ 0.15; at higher values the default parameters of PYTHIA give a satisfactory description of the data. This suggests a need for further study of fragmentation at low z, where large numbers of particles are found but where their association with jets may be less well defined than at high z.

The fragmentation functions determined using inclusive photoproduced jets are found to be in agreement with calculations from Binnewies et al. to within the uncertainty of the calculation as applied to the present data. A close similarity is seen between the present $h^{\pm}$ fragmentation functions in the range $0.15 < z_L < 0.7$ and those observed in $p\bar{p}$ scattering. Fragmentation functions have also been extracted for $h^{\pm}$ and K^0 in direct photoproduced jets, and are compared with corresponding data from e^+e^- annihilation and from deep inelastic scattering. Agreement is good for $z_E > 0.1$ and $z_E > 0.15$ for $h^{\pm}$ and K^0 respectively. This, together with the agreement found in this region with PYTHIA, represents a confirmation of the idea of a universally valid description of parton fragmentation.

Acknowledgements. We thank the DESY directorate and staff for their continued support and encouragement, and likewise the HERA machine group for their excellent efforts in operating HERA. We are grateful to J. Binnewies for helpful conversations and for making numerical calculations available.

References

1. H1 Collab., T. Ahmed et al., Phys. Lett. **B297** (1992) 205; H1 Collab., I. Abt et al., Phys. Lett. **B314** (1993) 436; H1 Collab., C. Adloff et al., Eur. Phys. J. **C1** (1998) 97
2. H1 Collab., S. Aid et al., Z. Phys. **C70** (1996) 17
3. ZEUS Collab., M. Derrick et al., Phys. Lett. **B293** (1992) 465; ZEUS Collab., M. Derrick et al., Phys. Lett. **B322** (1994) 287
4. ZEUS Collab., M. Derrick et al., Phys. Lett. **B342** (1995) 417
5. ZEUS Collab., M. Derrick et al., Phys. Lett. **B348** (1995) 665; ZEUS Collab., M. Derrick et al., Phys. Lett. **B384** (1996) 401
6. R.J. Cashmore, proc. Physics in Collision **3** (1983) 167
7. ZEUS Collab., M. Derrick et al., Z. Phys. **C68** (1995) 29
8. H1 Collab., S. Aid et al., Nucl. Phys. **B480** (1996) 3
9. H1 Collab., C. Adloff et al., Nucl. Phys. **B504** (1997) 3
10. ZEUS Collab., J. Breitweg et al., Phys. Lett. **B414** (1997) 428
11. H.-U. Bengtsson, T. Sjöstrand, Comp. Phys. Comm. **46** (1987) 43; T. Sjöstrand, CERN-TH.6488/92, Comp. Phys. Comm. **82** (1994) 74
12. T. Sjöstrand, M. van Zijl, Phys. Rev. **D36** (1987) 2019; G. Schuler, T. Sjöstrand, Phys. Lett. **B300** (1993) 169, Nucl. Phys. **B407** (1993) 539; J.M. Butterworth, J.R. Forshaw, J. Phys. **G19** (1993) 1657; J.M. Butterworth, J.R. Forshaw, M.H. Seymour, Z. Phys. **C 72** (1996) 637
13. ZEUS Collab., M. Derrick et al., Z. Phys. **C67** (1995) 93
14. E665 Collab., M.R Adams et al., Z. Phys. **C61** (1994) 539
15. DELPHI Collab., P. Abreu et al., Z. Phys. **C65** (1995) 587
16. H1 Collab., C. Adloff et al., Z. Phys. **C76** (1997) 213
17. J. Binnewies, G. Kramer, B.A. Kniehl, Phys. Rev. **D52** (1995) 4947, Phys. Rev. **D53** (1996) 3573; J. Binnewies, priv. comm.
18. MARK II Collab., H. Schellman et al., Phys. Rev. **D31** (1985) R3013; ALEPH Collab., D. Buskulic et al., Z. Phys. **C64** (1994) 361, and other work cited in [17]
19. ZEUS Collab., M. Derrick et al., Phys. Lett. **B297** (1992) 404; ZEUS Collab., M. Derrick et al., Phys. Lett. **B303** (1993) 183
20. N. Harnew et al., Nucl. Instr. Meth. **A279** (1989) 290; B. Foster et al., Nucl. Phys. B(Proc. Suppl.) **32** (1993) 181, Nucl. Instr. Meth. **A338** (1994) 254
21. C. Alvisi et al., Nucl. Instr. Meth. **A305** (1991) 30
22. A. Andresen et al., Nucl. Instr. Meth. **A309** (1991) 101; A. Bernstein et al., Nucl. Instr. Meth. **A336** (1993) 23; A. Caldwell et al., Nucl. Instr. Meth. **A321** (1992) 356
23. J. Huth et al., in proc. 1990 DPF Summer Study on High Energy Physics, Snowmass, Colorado, ed. E.L. Berger (World Scientific, Singapore, 1992) 134
24. Particle Data Group, R.M. Barnett et al., Phys. Rev. **D54** (1996)
25. A.S. Wilson, Ph. D. Thesis, University of Glasgow (1997); J.P. Fernández, Ph. D. Thesis, Universidad Autónoma de Madrid (1998)
26. G. Marchesini et al., Comp. Phys. Comm. **67** (1992) 465
27. ZEUS Collab., M. Derrick et al., Phys. Lett. **B348** (1995) 665
28. ZEUS Collab., M. Derrick et al., Phys. Lett. **B384** (1996) 401, Phys. Lett. **B369** (1996) 55
29. R. Brun et al., CERN DD/FF/84-1 (1987)
30. M. Glück, E. Reya, A. Vogt, Phys. Rev. **D46** (1992) 1973; H Plothow-Besch, Comp. Phys. Comm. **75** (1993) 396
31. A.D. Martin, R.G. Roberts, W.J. Stirling, Phys. Rev. **D 50** (1994) 6734
32. D.H. Saxon, in High Energy Electron-Positron Physics, eds. A. Ali, P. Söding, World Scientific (1988) 539
33. P. Aurenche et al., Z. Phys. **C64** (1994) 621
34. H. Abramowicz, K. Charchuła, A. Levy, Phys. Lett. **B269** (1991) 458
35. L.E. Gordon, J.K. Storrow, Z. Phys. **C56** (1992) 307
36. CDF Collab., F. Abe et al., Phys. Rev. Lett. **65** (1990) 968
37. TASSO Collab., W. Braunschweig et al., Z. Phys. **C47** (1990) 187
38. M. Basile et al., Nuov. Cim. **A79** (1984) 1
39. TASSO Collab., W. Braunschweig et al., Z. Phys. **C47** (1990) 167
40. HRS Collab., S. Abachi et al., Phys. Rev. **D40** (1989) 706